

ISTITUTO NAZIONALE DI FISICA NUCLEARE

Sezione di Milano

INFN/AE-84/5
13 Luglio 1984

G.Barbiellini, P.Buksh, G.Cecchet, J.Y.Hemery,
F.Lemeilleur, P.G.Rancoita, G.Vismara and A.
Seidman : SILICON DETECTORS AND ASSOCIATED
ELECTRONICS ORIENTED TO CALORIMETRY

Istituto Nazionale di Fisica Nucleare
Sezione di Milano

INFN/AE-84/5
13 Luglio 1984

Silicon detectors and associated electronics oriented to calorimetry

G. Barbiellini¹⁾, P. Buksh²⁾, G. Cecchet³⁾,
J. Y. Hemery²⁾, F. Lemeilleur²⁾, P. G. Rancoita⁴⁾,
G. Vismara²⁾, A. Seidman⁵⁾,

Abstract: In electromagnetic calorimetry large-size silicon detectors, employing relative low-resistivity material, can be used. The improvement in the leakage current performance of these devices enables to have mean depleted layers widths varying less than 0.3%. The low noise large capacitance oriented electronics provides a good signal-to-noise ratio for single relativistic particles traversing such a large area detector.

invited paper to the
Topical Seminar on Perspectives on Experimental Apparatus
at Future High Energy Machines
S. Miniato (Italy), 21-25 May 1984

-
- 1) Lab. Naz. de INFN, Frascati (Italy) and CERN
 - 2) CERN, Geneva, Switzerland
 - 3) INFN-Milano and Pavia, Italy
 - 4) INFN-Milano, Italy
 - 5) Tel-Aviv University, Ramat-Aviv, Israel

1. Introduction

Silicon detectors are currently a major instrument in high-energy physics experiments (for a review on the subject see [1] and [2]). They are attractive because they i) achieve high-resolution (the currently used microstrip detectors have a pitch strip of 20-50 μm), ii) are fast devices (the transit time is less than 10-20nsec), iii) operate in strong magnetic fields, in vacuum and iv) are adequate for experiments with geometric constraints. So far in high-energy physics experiments silicon detectors have been employed mainly as vertex detectors. However they can find application in calorimetry[3]-[5].

In electromagnetic and/or hadronic calorimetry a number of large-size silicon detectors are likely to be used. Inexpensive counters operated as not fully depleted (or quasi depleted) devices can be manufactured[5]. The depleted layer is between 100-200 μm and the active area is about 25cm² (for 3" wafers) and about 50cm² (for 4" wafers). Thus they require an associated electronics oriented to high (1-3nF) input capacitances.

In calorimetry, the energy scale of individual active layers is usually defined by calibrating the device with single non-showering relativistic particles. Thus the associated electronics needs to have a good performance both for calibration conditions (single relativistic particles traversing the device) and for showering conditions.

This paper presents the performance of the improved versions of both the low cost silicon detectors and its associated electronics.

2. High input capacitance oriented electronics

Two noise sources, serial and parallel, contribute to the total noise in different ratios as function of the input detector capacitance, C_D . The serial (current) noise is predominant at small input capacitance whilst the parallel (voltage) noise is bigger at large capacitance. In our application, where the detector capacitance exceeds 1nF considerably, voltage noise has to be kept very small (<1 nV/ $\sqrt{\text{Hz}}$).

We have performed tests with both FETs and bipolar transistors. We concluded that by using FETs with $g_m > 30\text{mA/V}$ the noise figure is better up to 3nF as compared to bipolar transistors. Above 3nF, the use of

bipolar transistors in the input stage seems to be appropriate.

The employed hybrid preamplifier[6] offers a better performance than the previously developed preamplifier[5] and most of the commercial ones[7]. The cascode frond-end stage (fig 1) uses a very high transconductance FET (Toshiba ZSK147). Special care has been dedicated to the choise of the current-source generator and the grounded base transistor. In Table 1, a summary of the preamplifier characteristics is given.

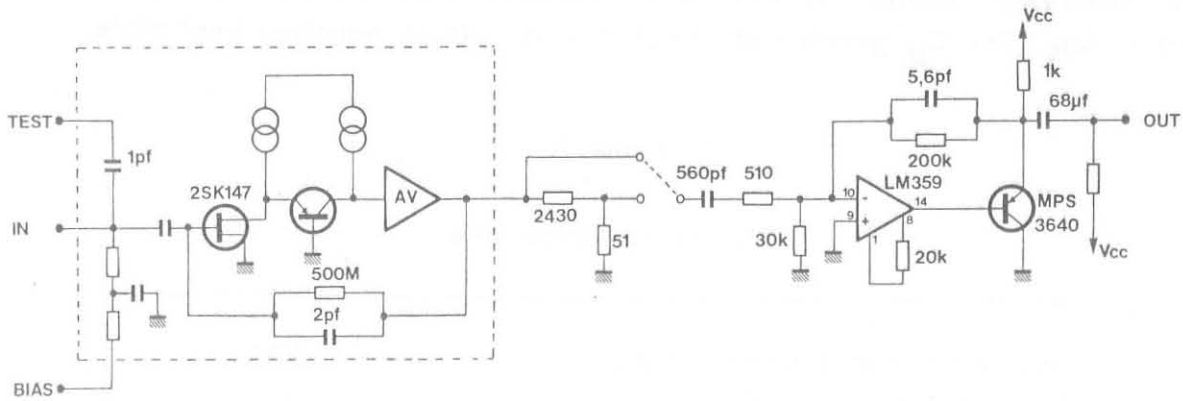


FIG 1 : Preamplifier lay-out

Table 1

Preamplifier specifications

Z _{in}	300kΩ/3 nF
Open loop gain.....	>63 dB
t _{rise}	<10 ns
T _f =R _f C _f	1 ms
Sensitivity.....	0.5 mV/fC
Equivalent noise charge.....	<[0.05+0.47/nF] fC at T _S =1µs
Output impedance.....	<2 Ω
Max. output voltage.....	+8 V/40 mA; -5V/-1mA
Slew rate.....	2500V/µs; -50V/µs
Power supply.....	+12V/6mA; -12V/-1.5mA
Power consumption.....	90mW

The use of a Norton amplifier (1/2LM359), which provides a large gain-band width, enabled a shaping time of $1\mu\text{s}$ and voltage gain of 200 with a single stage. The shaping is obtained by simple integration and differentiation. A PNP emitter follower has been introduced in the feed-back path in order to drive 50Ω lines up to 2V with good linearity. The large dynamic range from a single relativistic particle (calibration conditions) to the showering condition is obtained partially by the ADC dynamic range and by a resistive attenuator with a factor of 50 located between the preamplifier and the amplifier. The equivalent input noise is affected by this attenuator mainly at low input capacitances, where the preamplifier gain is low. For C_D greater of about 1nF its effect becomes negligible.

Table 2

Shaper specifications

Equivalent input noise voltage.....	$3\mu\text{V}$
Shaping time= $T_{\text{diff}}=T_{\text{int}}$	$1\mu\text{s}$
Gain= adjustable in two steps.....	170 and 3.4
Output impedance.....	$<2\Omega$
Max output voltage.....	-5V/50 Ω
Power supply.....	+12V/19mA
Power consumption.....	230mW

The behaviour of the electronics as a function of the input capacitance has been measured by feeding a calibrated step function through a 10pF test capacitance. The Equivalent Noise Charge (ENC) has been determined (fig 2) by using a Tekronix 7854 digital memory oscilloscope which has a built-in root mean square function, averaging over 20000 samples.

In fig 3, the ENC versus the detector capacitance is given. We estimate that

$$\text{ENC}=0.046+0.567C_i \quad [\text{fC}]$$

where C_i is the input capacitance in nF. The standard deviation of the electronics noise contribution is about 1.0keV at $C_D=0.\text{pF}$ and 17.6keV at

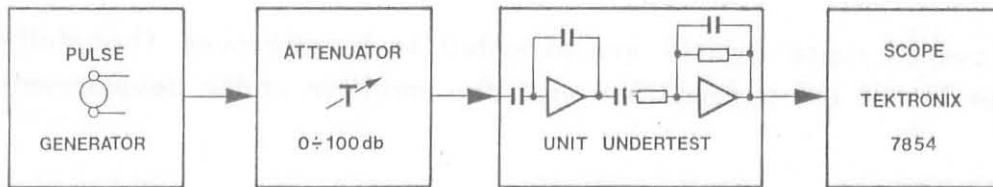


FIG 2 : Set-up for measuring the equivalent noise charge

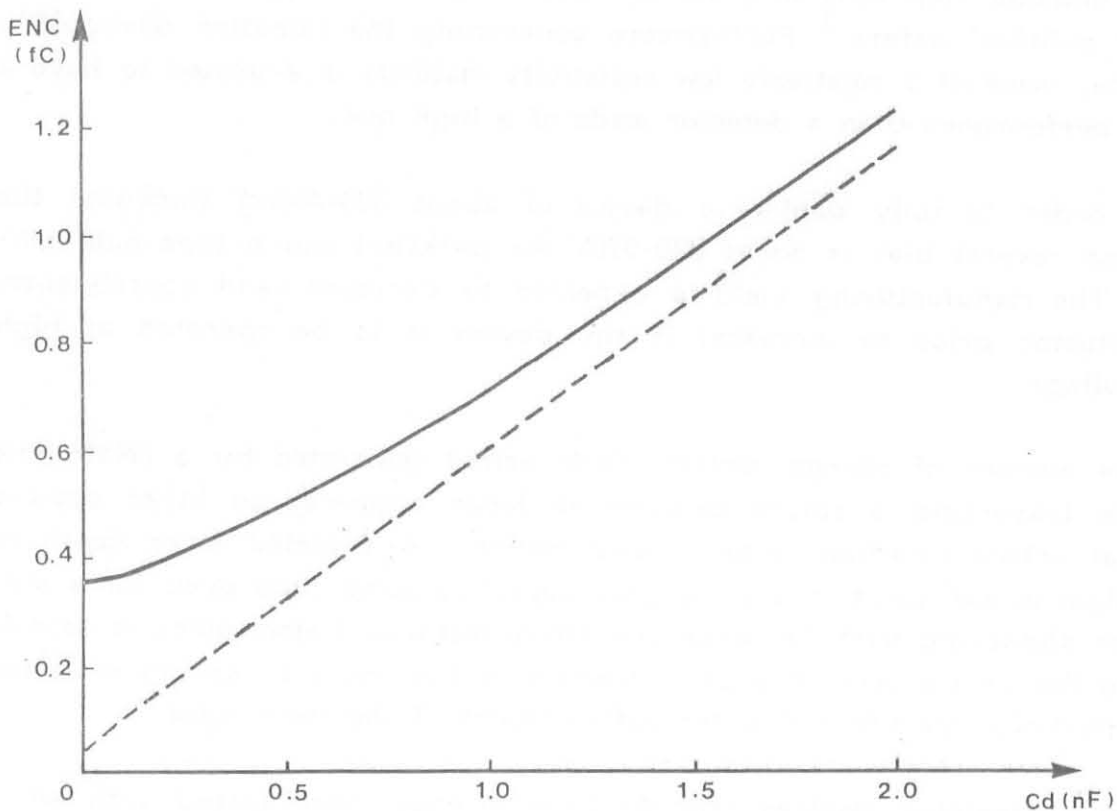


FIG 3 : Equivalent noise charge (ENC) vs the input capacitance. The dashed line is without the attenuator and the full line is with the factor 50 attenuator between the preamplifier and the amplifier.

$C_d \approx 1.3 \text{ nF}$. When the attenuator is introduced, the shaper noise contribution becomes predominant at low capacitance and for $C_d > 300 \text{ pF}$

$$\text{ENC} = 0.322 + 0.414 C_i \quad [\text{fC}]$$

The expected standard deviation of the electronics noise contribution is about 19.4 keV for $C_d \approx 1.3 \text{ nF}$.

These overall noise figures are expected to be improved (hopefully) in the new version of the preamplifier and the amplifier under development.

3. Large area silicon detectors

Nowadays, large area silicon detectors can be manufactured by using 3" or 4" wafers. The active area enlargement is accompanied by an increase of the detector thickness in order to have a sufficiently good device rigidity for polished wafers.¹ Furthermore concerning the radiation damage[8], a device, made of a relatively low resistivity material is expected to have a better performance than a detector made of a high one.

In order to fully deplete a device of about 300-400 μ m thickness the required reverse bias is about 320-570V for $\rho \approx 1\text{k}\Omega\text{cm}$ and n-type bulk silicon. The manufacturing yield is expected to decrease (and consequently the detector price to increase) if the device is to be operated at high bias-voltage.

The number of charge carriers (e-h pairs) generated by a relativistic particle traversing a silicon detector is large compared to other devices used as active sampling layer in calorimetry. A depleted layer depth of 150-300 μ m is sufficient to allow a good signal-to-noise ratio even for a single non showering particle, when the above mentioned electronics is associated to the device (see chap.2). However in the usual showering condition many particles are traversing the active layers of the calorimeter.

The undepleted devices (fig 4) have already been tested with short integrating electronics. It has been proved that they have an equal performance compared to fully depleted detectors with the same width of space charge region[9].

A long integrating time of the associated electronics provides a signal

¹ It is under development a detector made of a 4" wafer etched, but not polished. In this way detectors with a thickness of about 220 μ m are obtained from 4" wafers. However they will have a thickness variation of $\pm 15\mu\text{m}$ across the active area.

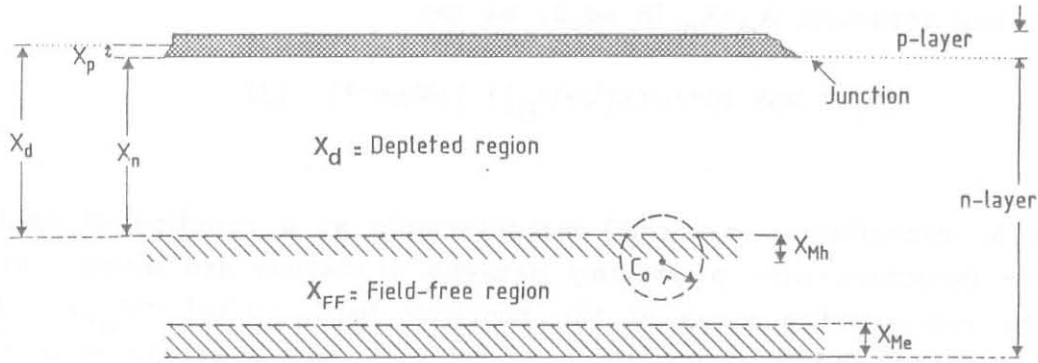


FIG 4 : Sectional view of an undepleted n-type bulk silicon detector: X_{Me} is the layer from which electrons migrate towards the positive electrode, X_{Mh} is the layer from which the holes migrate into the space charge layer. The overall depleted layer, X_d , is the sum of the space charge layer in the p-zone, X_p , and in the n-zone, X_n . The diffusion length, r , of the carrier C_0 depends on the effective collection time.

with a contribution due to charge which migrates from the field-free region. This charge corresponds to the collection of e-h pairs created in 25-50 μ m inside the field-free zone for a collection time of about 0.5-1.0 μ s [10].

3.1. Undepleted detectors

As well known, for a depleted layer much larger than which is generated by the built-in voltage, a step-junction behaviour is expected. Thus, the relationship between the depleted layer in the bulk n-type silicon, X_n , and the resistivity is

$$X_n \approx \sqrt{(2\epsilon_{Si}\epsilon_0\mu_n\rho[V+V_B])} \quad (1)$$

where V is the externally applied reverse-bias, ϵ_0 is the free space permittivity, ϵ_{Si} is the dielectric constant of silicon and μ_n is the electron mobility. In the case $V \gg V_B$, we have $X_n \approx 0.529 \cdot 10^{-4} \sqrt{(\rho V)}$ [cm].

The depletion layer capacitance per unit-area, C_T , for plane and step junction is

$$C_T = \epsilon_{Si}\epsilon_0/X_d \approx 1.0359/X_d \text{ [pFcm}^{-2}] \quad (2)$$

From eq.1 and assuming $X_d \approx X_n$ in eq.2, we get

$$C_T \approx 1.958 \cdot 10^4 / \sqrt{\rho[V+V_B]} \text{ [pFcm}^{-2}] \quad (3)$$

In fig 5, capacitance (per cm²) measurements as a function of applied voltage for detectors with ρ varying between 1-18k Ω cm are given. It is possible to estimate the slope of the function $\lg(C_T) = f(\lg[V+V_B])$. The slope is expected to be independent of $[V+V_B]$ and equal to -0.5 (see eq.3). In Table 3, the values of the slope are shown assuming $V_B = 0$ and $V_B = 0.5$ V. An agreement, of better than 0.3%, with the expected slope is obtained for $V_B = 0.5$ V. This value of V_B is agreement with the expected built-in voltage of detectors whose resistivity is between of 1-18k Ω cm. These measurements indicate no strong systematic resistivity variation across the detector. In the latter case, the capacitance dependence on the reverse bias is no longer following a square root behaviour.

A systematic study regarding the depleted layer variation across the detectors has been performed by exposing the devices to a 100GeV/c proton beam at CERN-SPS. The detectors were operated with a depleted region of

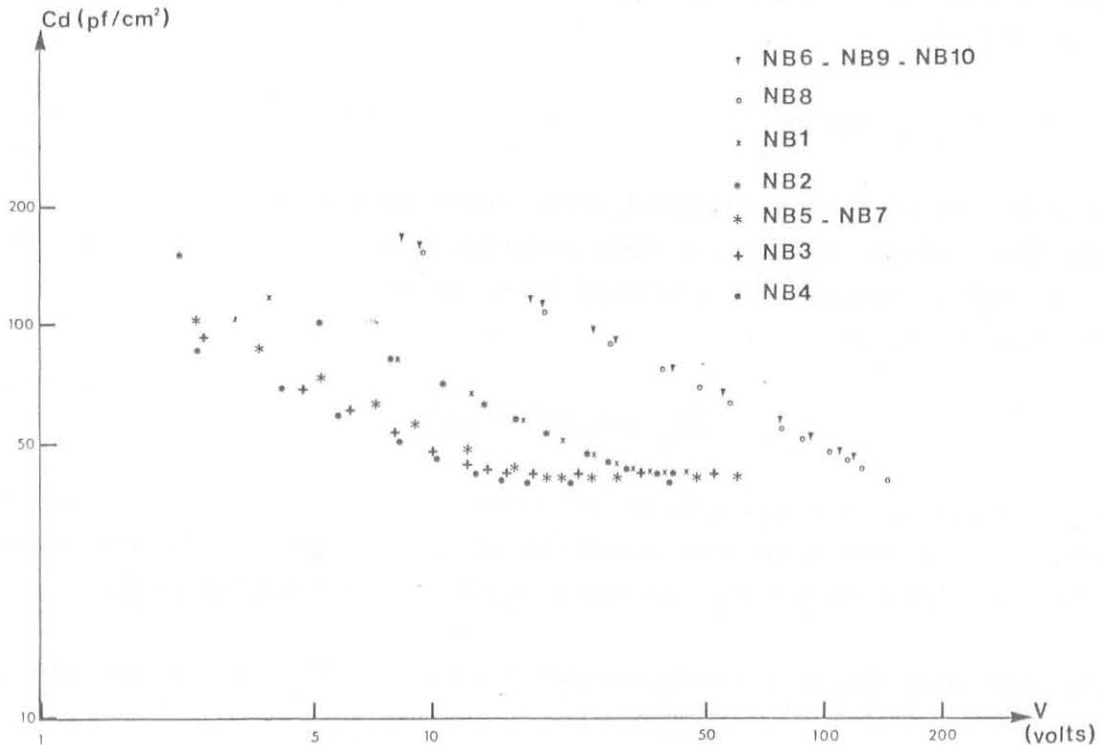


FIG 5 : Capacitance (per cm²) vs the applied reverse bias for a sample of ten detectors. Each device has an active area of 25cm².

Table 3

Slope vs built-in voltage and resistivity

	$V_B=0.V$	$V_B=0.5V$	$\rho[k\Omega cm]$
NB1	-0.482	-0.500	6.8
NB2	-0.480	-0.503	7.0
NB3	-0.458	-0.489	16.7
NB4	-0.455	-0.493	18.7
NB5	-0.480	-0.504	13.2
NB6	-0.492	-0.502	1.6
NB7	-0.478	-0.502	13.2
NB8	-0.488	-0.497	1.6
NB9	-0.489	-0.499	1.6
NB10	-0.491	-0.499	1.6

$\approx 200\mu m$, i.e. a capacitance of $1.3nF$. The energy loss spectra sensed by the devices were recorded as a function of the proton impact position, defined by a movable scintillator counter of $0.5 \times 0.5 cm^2$ area. The energy loss spectra were fitted to a Landau distribution convolved by a gaussian function[11]. For small variations around any fixed sensitive width (in this case $\approx 200\mu m$), the most probable energy loss is linearly proportional to the width of the actual depleted layer of the detector. In this way the variation of the depleted region, ΔX_D , across the the detector has been determined to be $|\Delta X_D| = (5.8 \pm 2.6)\mu m$ for $X_D = 200\mu m$.

3.2. Leakage current time dependence

An important requirement for a stable calorimeter and in order to keep the absolute calibration at better than 1% is the low value of the leakage current. In this way the energy resolution is not degraded and a negligible variation of the depleted layer depth is obtained when the device is operated not fully depleted.

A great deal of development has allowed these low-price oriented devices² to have a leakage current in the range of $17-80nA/cm^2$ (for compari-

² They are manufactured by Micron Semiconductor (U.K.)

son see[5]).

The leakage current variation of a few 25cm² active area devices has been monitored over a few days. It was found that the leakage current is practically following the room temperature variation. The relative variation ($[\text{maximum}-\text{minimum}]/\text{minimum}$) is about 7-12%. Thus the effect on the reverse bias is not greater than a fraction of a Volt when a typical 1-10M Ω series resistance is used to supply the current. Furthermore no major degrading of the energy resolution is expected.

3.3. Radition damage in high energy machines environment

Although the size of silicon detectors is relatively small, good energy resolution can be obtained and they can be employed under conditions that other detectors cannot be used. They can also be used for ionization measurement from individual particles, for high precision position detection, for event multiplicity measurement, etc. The effect of radiation on silicon detectors is, therefore, of interest to high-energy physicists.

Collisions of ionizing particles and of secondary electrons may lead to the displacement or desintegration of atoms in the silicon cristal, causing damage to it. The main effect - head on collision - requires more than 200 keV in order to displace an atom. Vacancies left behind by displaced atoms form defects as localized energy levels in the forbidden band-gap, become recombination centres. The interstitial (ejected) silicon atom migrates either to dislocations in the crystal or to the crystal boundary.

Despite the progress made in the study of lattice damage introduced in silicon during ion implantation, very little is known about the nature and characteristics of specific defects [12]. It was found that the bombardment of silicon wafers with ions results in the production of defects which act as efficient recombination centres [13].

The amount of radiation-induced defects increases with the duration of irradiation, causing deterioration in the performance of the silicon detectors. As long as it is smaller than the built-in charge density of the detector ($10^{14} - 10^{16} \text{ cm}^{-3}$), though degraded, it can still be used.

The above mentioned defects cause an increase in the reverse current and a decrease of the minority carrier lifetime of silicon detectors, thus causing an increase of noise. The radiation-induced increase in leakage

current is roughly proportional to the increase of the fluence.

Other effects are charge-loss caused by recombination centres and the need of increased bias-voltage for full depletion because of the increased leakage current (which increases with irradiation dose). Unlike the bias voltage, the leakage current does not remain constant with time.

Since silicon detector systems may be complex and expensive, it is important to establish the limits imposed by radiation damage on detector lifetime. But, so far, there are few published results which could be practically useful.

A study of the effects of muon flux was made [14], using different detectors and continuously monitoring them via their leakage current compensation and via comparison with calibration detectors which were most of the time kept outside the radiation. Results are presented in fig.6. It can be seen that the degradation, measured by current and detector noise, is worse for high resistivity n-type silicon detectors.

A more recent study [8] was performed on ion-implanted silicon-junction detectors which were exposed to doses of high-energy hadrons produced by 24 GeV/c protons at CERN Proton Synchrotron up to the fluences of 8.3×10^{13} particles cm^{-2} . It was found that in order to obtain a working detector after irradiation, the bias voltage must be increased to obtain full depletion and charge collection from the intensely disordered small volumes created by the radiation [1]. Also a considerable increase in leakage current occurred. It was found that the performance of the detector itself in responding to high-energy particles is not impaired, provided electronics with short rise-time is used. The constancy of charge collection indicates that the detector with its electronic is sensing and responding in the same way to the same energy loss (fig.7). The peak position and the full width at half maximum, once subtracted the noise contribution, were found to be independent of the fluences (fig 8 and 9). Thus, up to at least the maximum fluence of this study, silicon detectors can be used as live targets in high-rate, high-energy physics experiments. This conclusion is valid as long as the energy resolution is not required to be better than 15 keV. These results can be expected to be valid also for surface-barrier and thermally diffused silicon detectors, since the physical mechanism of damage seems not to depend on the nature of the junction.

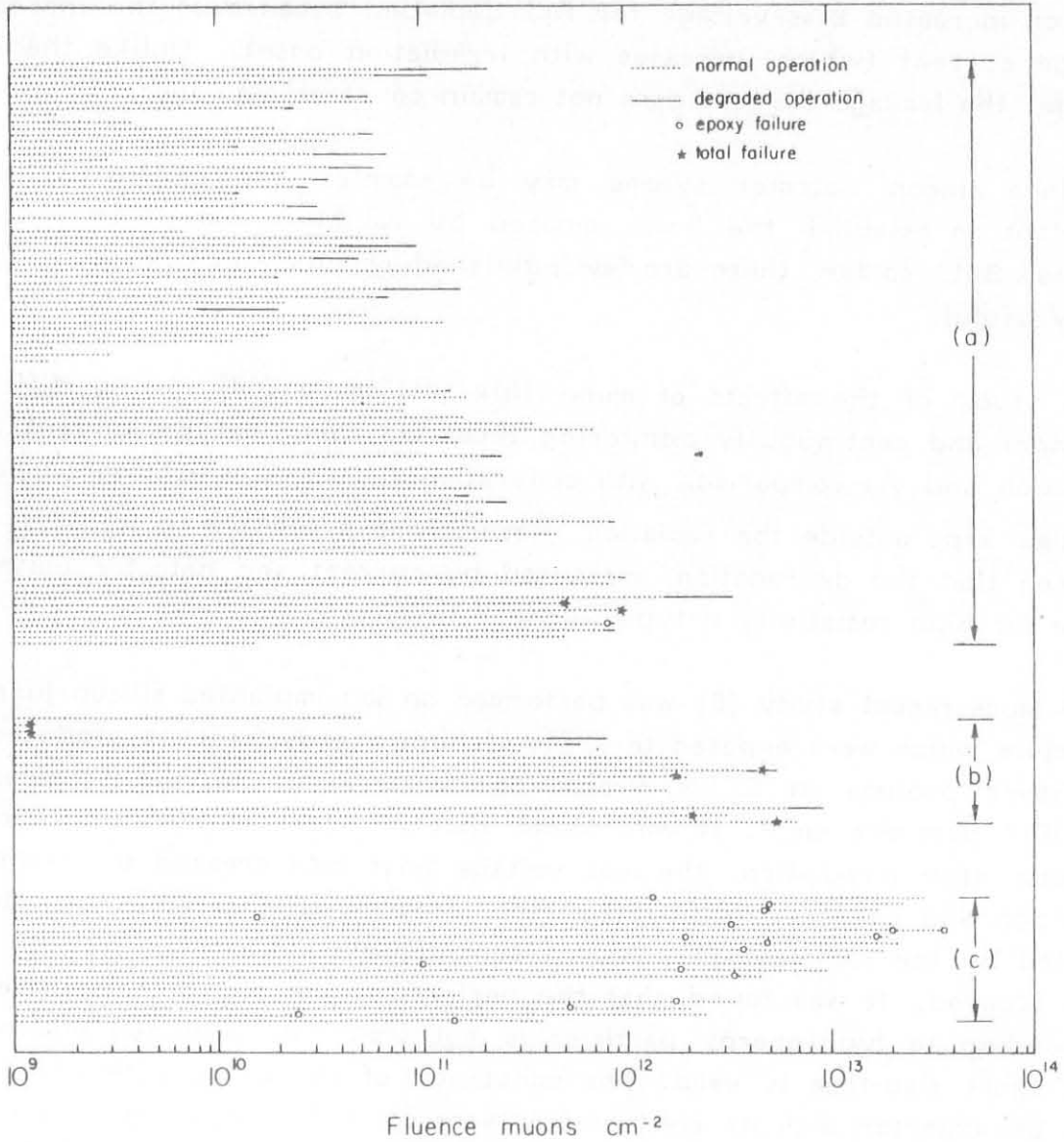


FIG 6 : The total muon dose (number of muons per cm^2) received by the silicon detectors. The operational status of each detector is indicated. For some detectors complete failure (*) occurred, others had recoverable epoxy failure (o), still others could continue operations for some time, while degraded (-), due to high noise, high leakage current or incomplete charge collection. The class (a) detectors are n-type surface barrier, from top to bottom in order of decreasing resistivity; (b) are ion implanted detectors of $1\text{k}\Omega\text{cm}$ Si; (c) are p-type diffused of $2\text{k}\Omega\text{cm}$.

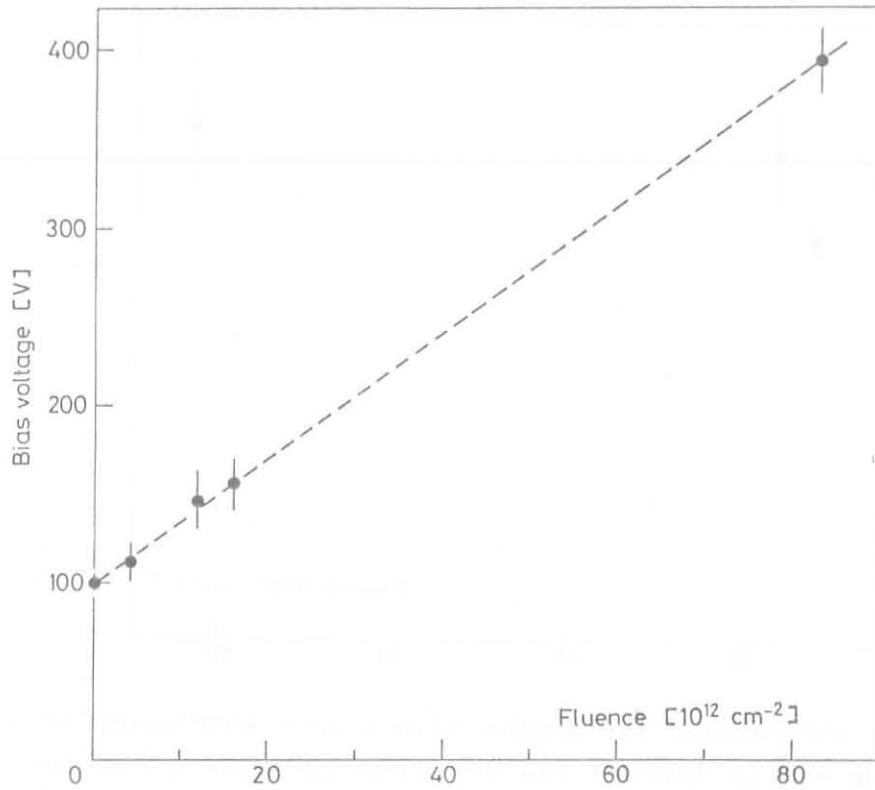


FIG 7 : Bias voltage across detector for full depletion and charge collection vs. fluence.

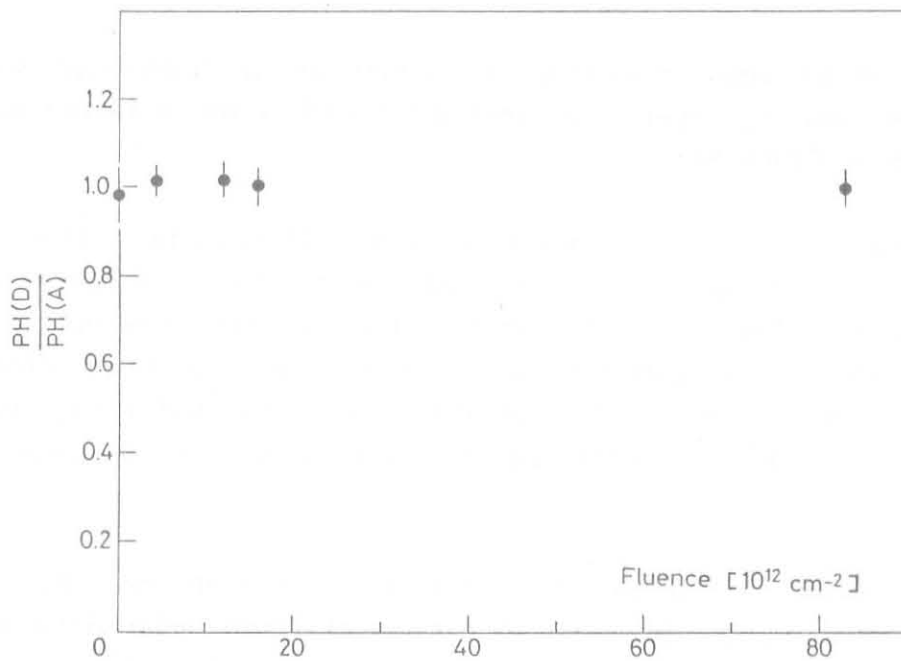


FIG 8 : Ratio of the most probable energy loss of irradiated detector D over a nonirradiated monitoring detector A vs. fluence.

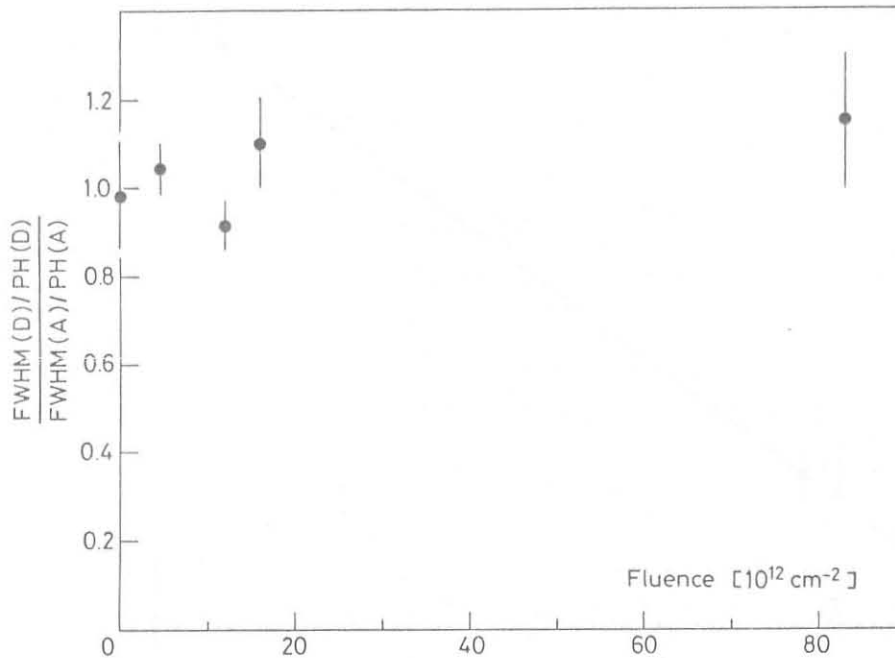


FIG 9 : Ratio of the relative full widths (FWHM with subtracted noise over the most probable energy loss) of the irradiated detector D and the nonirradiated detector A vs. fluence.

4. Si-Calorimeter

A prototype of an electromagnetic calorimeter using undepleted silicon devices as active sampling layers has been built and is being tested at the X7 electron beam at CERN-SPS.

The calorimeter consists of 24 radiation lengths of tungsten. The active sampling detectors, of $5 \times 5 \text{ cm}^2$ area, are located every two radiation lengths of tungsten (fig 10). The interlayer distance between two adjacent passive absorbers is 1.6mm. The detectors are operated with a mean depleted layer width of $200 \mu\text{m}$. The variation of their mean depleted zone, due to the variation of the leakage current, was found to be 0.3% on average, and never exceeding 1%.

The energy scale calibration, for each individual device, has been carried out by exposing the detectors to a beam of single relativistic particles (namely 100 GeV protons) and taking away the tungsten plates. In fig 11, the energy loss spectrum sensed by a detector is shown. The full line is the fit to a Landau distribution convolved by a gaussian function. The

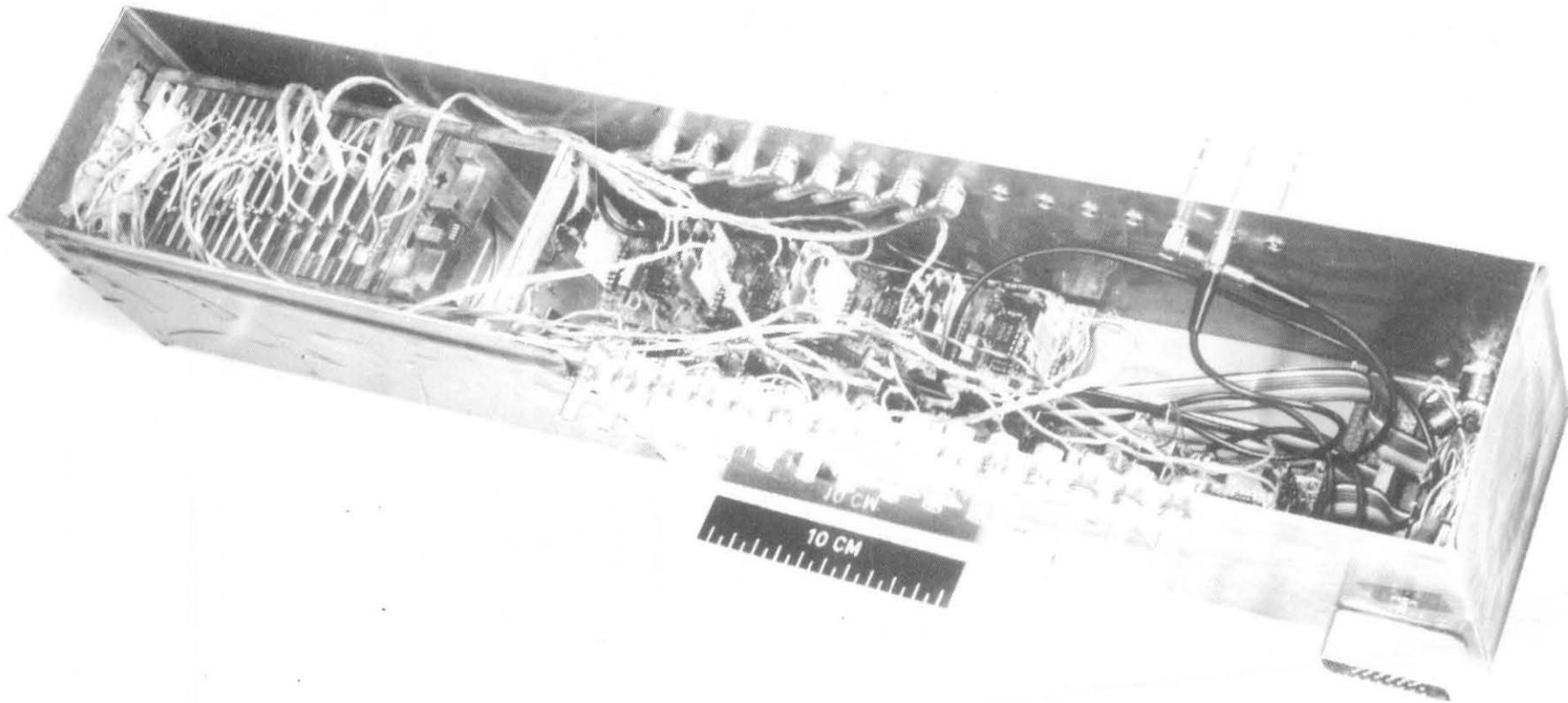


FIG 10: Prtotype of an electromagnetic calorimeter employing silicon detectors as active sampling devices. The solid state devices have an active area of $5 \times 5 \text{ cm}^2$ and a depleted width of $200 \mu\text{m}$.

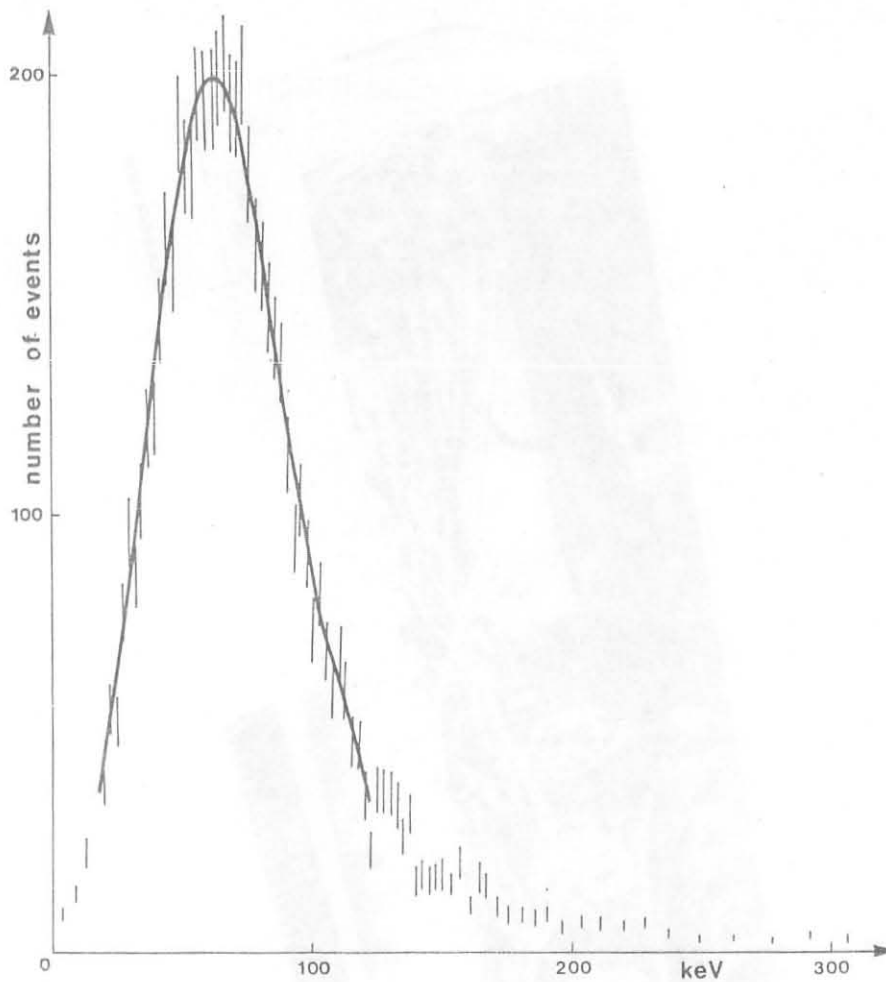


FIG 11: Energy loss spectrum of a relativistic proton traversing a large ($5 \times 5 \text{cm}^2$) area silicon detector depleted at $200 \mu\text{m}$. The most probable energy loss is 56keV and the standard deviation of the gaussian noise contribution is 20.8keV . The full line is the fit the a Landau distribution convolved with a gaussian function.

standard deviation of the gaussian noise distribution was 26.7KeV on average. This value takes into account the contributions due to electronics, detector and cabling.

In front of the calorimeter, a small silicon detector of $0.5 \times 0.5 \text{cm}^2$ is located. Thus only electrons impinging in the centre of the device are triggered. In this way a fully lateral containment is expected.³

³ The lateral shower development is contained at about 95% (for tungsten) in a cylinder with 2.5cm of radius.

The tests regarding the energy linearity and resolution are expected to be performed in the X7 electron beam soon.

5. Conclusion

The improvement of the leakage current performance of the large area silicon detectors has enabled to operate undepleted devices with a highly stable depleted layer width.

The currently employed electronics seems to be adequate in order to calibrate the individual active layer of the calorimeter with single non showering relativistic particles.

ACKNOWLEDGMENTS

The authors are indebted to C.Leroy for collaboration in preparing the experimental test.

References

- [1] P.G.Rancoita and A.Seidman, *La Rivista del Nuovo Cimento* vol.5, Nu. 7 (1982)
- [2] P.G.Rancoita, *Journal of Physics G* 10 (1984), 299
- [3] P.G.Rancoita, U.Koetz, R.Klanner and H.Lierl, *Proc. of the Workshop on Experimentation at HERA machine*, (Amsterdam 9-11 June 1983), DESY HERA 83/20, p 105
- [4] G.Barbiellini, G.Cecchet, J.Y.Hemery, F.Lemeilleur, P.G.Rancoita, A.Seidman and M.Zilka, *Silicon/tungsten calorimeter as luminosity monitor*, contributed paper No.102 to the *International Europhysics Conference on High Energy Physics* (Brighton 20-27 July, 1983), INFN/TC-83/15 (20.9.1983)

[5] P.G.Rancoita and A.Seidman, Silicon detectors in calorimetry, INFN/AE-84/1 (12.1.1984), to appear in Nucl. Instr. and Meth. (1984)

[6] M.Goyot, An hybrid low power and low noise charge sensitive preamplifier for large capacitance photodiode, talk given at L3 BGO meeting, CERN 24-25 January 1984

[7] G.Vismara, Comparative measurements on charge preamplifiers for a large detector capacitance, to appear as CERN-LEP division note (1984).

[8] P.Borgeaud, G.McEwen, P.G.Rancoita and A.Seidman, Nucl. Instr. and Meth. 211 (1983), 363

[9] G.Barbiellini and P.G.Rancoita, A luminosity monitor for LEP using electromagnetic calorimeters: the silicon/lead sandwich, CERN-EP Internal Report 83-01, 6.1.83

[10] N.Croitoru, P.G.Rancoita and A.Seidman, Charge migration contribution to the sensitive layer of a silicon detector, submitted to Nucl. Instr. and Meth. (1984)

[11] S.Hancock, F.James, J.Movchet, P.G.Rancoita and L.VanRossum, Phys. Rev. A28 (1983), 615

[12] L.C.Kimerling and J.M.Poate, Proc. of Int. Conf. on lattice defects in semiconductors, Freiburg (1974), Inst. Phys. Ser No.23, London-Bristol, 1975, p 126

[13] V.D.Trachev et al., Rad. Effects 49 (1980), 133

[14] E.Heijne, Radiation Damage: experience with silicon detectors in high-energy particle beams at CERN, Proc. Miniaturization of detectors, Pisa Conf. 1980, ed A.Stefanini, Plenum Press London 1983.